ELSEVIER

Nuclear Physics A 707 (2002) 561–576

NUCLEAR PHYSICS A

www.elsevier.com/locate/npe

Neutrino–deuteron reactions at solar neutrino energies

S. Nakamura [a,*], T. Sato [a,b], S. Ando [b], T.-S. Park [b], F. Myhrer [b], V. Gudkov [b], K. Kubodera [b]

[a] *Department of Physics, Osaka University, Toyonaka, Osaka 560-0043, Japan*
[b] *Department of Physics and Astronomy, University of South Carolina, Columbia, SC 29208, USA*

Received 11 April 2002; accepted 1 May 2002

Abstract

In interpreting the SNO experiments, accurate estimates of the νd reaction cross sections are of great importance. We improve the previous estimates of our group by updating some of its inputs and by taking into account the results of a recent effective-field-theoretical calculation. The new cross sections are slightly ($\sim 1\%$) larger than the previously reported values. It is shown to be reasonable to assign 1% uncertainty to the νd cross sections reported here; this error estimate does *not* include radiative corrections, for which we refer to the literature.

PACS: 25.30.Pt; 25.10.+s; 26.65.+t; 95.30.Cq

Keywords: Neutrino–deuteron reaction; Solar neutrino; Neutrino oscillations; Exchange current; Effective field theory

1. Introduction

The establishment of the Sudbury Neutrino Observatory (SNO) [1,2] has motivated intensive theoretical effort to make reliable estimates of the neutrino–deuteron reaction cross sections [3–6]. One of the primary experiments at SNO is the measurement of the solar neutrino flux. By observing the charged-current (CC) reaction, $\nu_e d \to e^- pp$, one can determine the flux of the solar electron-neutrinos while, by monitoring the neutral-current (NC) reaction, $\nu_x d \to \nu_x pn$ ($x = e$, μ or τ), one can determine the total flux of

* Corresponding author.
E-mail address: nakamura@kern.phys.sci.osaka-u.ac.jp (S. Nakamura).

0375-9474/02/$ – see front matter
PII: S0375-9474(02)00993-4

the solar neutrinos of any flavors. These features make SNO a unique facility for studying neutrino oscillations. SNO is also capable of monitoring the yield of the neutrino–electron elastic scattering (ES), $\nu_e e \to \nu_e e$, which also carries information on neutrino oscillations. The first report from SNO [2] was concerned with the measurements of the CC and ES processes. By combining the SNO data on the CC reaction with the Super-Kamiokande data on ES [7],[1] strong evidence for ν_e oscillations has been obtained [2]. It is to be noted that the sharpness of this important conclusion depends on the precision of theoretical estimates for the νd-reaction cross sections. In the present communication we wish to describe our attempt to improve the existing estimates.

We first give a brief survey of the theoretical estimates of the νd-reaction cross section that were used in the analysis in [2].[2] A highly successful method for describing nuclear responses to electroweak probes is to consider one-body impulse approximation (IA) terms and two-body exchange-current (EXC) terms acting on non-relativistic nuclear wave functions, with the EXC contributions derived from one-boson exchange diagrams [8]. We refer to this method as the standard nuclear physics approach (SNPA) [9].[3] The most elaborate calculation of the νd cross sections based on SNPA has been done by Nakamura et al. (NSGK) [5]. Since the νd reactions in the solar neutrino energy ($E_\nu \leqslant 20$ MeV) is dominated by the contribution of the space component, $\boldsymbol{A}$, of the axial current (A_μ), the theoretical precision of $\sigma_{\nu d}$ is controlled essentially by the accuracy with which one can calculate the nuclear matrix element of $\boldsymbol{A}$. Let us decompose $\boldsymbol{A}$ as $\boldsymbol{A} = \boldsymbol{A}_{\rm IA} + \boldsymbol{A}_{\rm EXC}$, where $\boldsymbol{A}_{\rm IA}$ and $\boldsymbol{A}_{\rm EXC}$ are the IA and EXC contributions, respectively. Since $\boldsymbol{A}_{\rm IA}$ is well known, the theoretical uncertainty is confined to $\boldsymbol{A}_{\rm EXC}$. Now, among the various terms contributing to $\boldsymbol{A}_{\rm EXC}$, the Δ-excitation current ($\boldsymbol{A}_\Delta$) gives the most important contribution [10], and $\boldsymbol{A}_\Delta$ involves the coupling constants for the $A_\mu N\Delta$ vertex, the $\pi N\Delta$ vertex and the $\rho N\Delta$ vertex, and the corresponding form factors. Although the quark model is believed to provide reasonable estimates for these coupling constants, it is at present impossible to test their individual values empirically; only the overall strength of the Δ-excitation current can be monitored with electroweak processes in a few-nucleon system. NSGK therefore considered two methods for controlling the strength of the Δ-excitation current. In one method, by exploiting the fact that the Δ-excitation current features in the $np \to \gamma d$ amplitude as well, its strength is determined so as to reproduce the $np \to \gamma d$ cross section. The second method uses the tritium β decay rate, Γ_t^β, and the strength of the Δ-excitation current is adjusted, as in Refs. [10,11], to reproduce the well-known experimental value of Γ_t^β. The first method was found to give $\sigma_{\nu d}$ about 3% larger than the second method, and NSGK adopted this 3% difference as a measure of uncertainty in their calculation based on SNPA.

Apart from SNPA, a new approach based on effective field theory (EFT) has been scoring great success in describing low-energy phenomena in few-nucleon systems [12–14]. Butler et al. (BCK) [6] applied EFT to the νd reactions, using the regularization

[1] The SNO data on ES is consistent with the Super-K data [7] but the latter has higher statistics.

[2] In what follows, $\sigma_{\nu d}^{\rm CC}$ and $\sigma_{\nu d}^{\rm NC}$ stand for the total cross sections (in the laboratory frame) for the CC and NC reactions, respectively; in referring to $\sigma_{\nu d}^{\rm CC}$and $\sigma_{\nu d}^{\rm NC}$ collectively, we use the generic symbol, $\sigma_{\nu d}$. The incident neutrino energy in the lab-frame will be denoted by E_ν.

[3] This approach was called the phenomenological Lagrangian approach (PhLA) in [5].

scheme called the power divergence subtraction (PDS) [15]. Their results agree with those of NSGK in the following sense. The EFT Lagrangian used by BCK involves one unknown low-energy constant (LEC), denoted by L_{1A}, which represents the strength of A_μ–four-nucleon contact coupling. BCK adjusted L_{1A} to optimize fit to the $\sigma_{\nu d}$ of NSGK and found that, after this optimization, the results of the EFT and SNPA calculations agree with each other within 1% over the entire solar-ν energy region. Furthermore, the best-fit value of L_{1A} turned out to be consistent with what one would expect from the "*naturalness*" argument [6]. The fact that the results of an ab initio calculation (modulo one free parameter) based on EFT are completely consistent with those of SNPA may be taken as evidence for the basic soundness of SNPA.

Having given a brief survey of the existing theoretical estimates of $\sigma_{\nu d}$, we now describe several points that need to be addressed for improving the estimates. We first note that, as pointed out by Beacom and Parke [16], the value of the axial coupling constant, g_A, used in NSGK is not the most updated one. This obvious deficiency needs to be remedied. Secondly, in their treatment of $\boldsymbol{A}_{\rm EXC}$, NSGK left out some sub-dominant diagrams, and therefore it is worthwhile to examine the consequences of using the full set of relevant Feynman diagrams [11]. Furthermore, NSGK adopted as their *standard run* the case in which the strength of the Δ-excitation current was adjusted to reproduce the measured $np \to \gamma d$ rate. However, the $np \to d\gamma$ reaction governed by the vector current cannot be considered as a better constraint than Γ_t^β for monitoring the effective strength of the $A_\mu N\Delta$ vertex relevant to the axial-vector transition. In the present work, therefore, we adopt as our standard choice the case in which $\boldsymbol{A}_{\rm EXC}$ is controlled by Γ_t^β. Thirdly, at the level of precision in question, radiative corrections become relevant [16–18]. In this communication, however, we do not address radiative corrections *per se* and simply refer to the literature on this issue [16–18]. A related problem is what value should be used for the weak coupling constant. One possibility is to use the standard Fermi constant, G_F, which has been derived from μ-decay and hence does not contain any hadron-related radiative corrections. Another possibility is to employ an effective coupling constant (denoted by G_F') that includes the so-called inner radiative corrections for nuclear β-decay. NSGK adopted the first choice. However, since the inner corrections are established reasonably well, it seems more natural to use G_F' instead of G_F. We therefore adopt here G_F' as the weak coupling constant (see below for more detail). An additional point that warrants a further study is the stability of the calculated value of $\sigma_{\nu d}$ against different choices of the NN interactions. NSGK investigated this aspect for a rather wide variety of modern high-quality NN interactions [19,20] and found the stability of $\sigma_{\nu d}$ at the 0.5% level. The interactions considered in NSGK, however, are all local potentials and have similar values of the deuteron D-state probability, P_D. Since the CD-Bonn potential [21] has a somewhat smaller value of P_D than the other modern high-quality NN potentials, we study here whether the stability persists with the use of the CD-Bonn potential.

Besides these improvements within the framework of SNPA, we present here a new comparison between SNPA and EFT. Park et al. [22–24] have developed an EFT approach wherein the electroweak transition operators are derived with a cut-off scheme EFT (à la Weinberg [12]) and the initial and final wave functions are obtained with the use of the high-quality phenomenological nuclear interactions. For convenience, we refer to this approach as EFT*. EFT* applied to the Gamow–Teller transitions contains one unknown

LEC denoted by $\hat{d}_R$, which plays a role similar to L_{1A} in BCK. In EFT*, however, one can determine $\hat{d}_R$ *directly* from Γ_t^β [24]. This allows a parameter-free calculation of $\sigma_{\nu d}$, and very recently Ando et al. have carried out this type of calculation [25]. We present a comparison between our new results based on SNPA and those based on EFT*, and we argue that good agreement between them renders further support for the robustness of $\sigma_{\nu d}$ obtained in SNPA. It will be seen that the new values of $\sigma_{\nu d}$ are close to those given in NSGK, but that a significant improvement in error estimates has been achieved.

2. Formalism

We study the total and differential cross sections for the CC and NC reactions of neutrinos and antineutrinos with the deuteron:

$$\nu_e + d \to e^- + p + p \quad \text{(CC)}, \tag{1}$$
$$\nu_x + d \to \nu_x + n + p \quad \text{(NC)}, \tag{2}$$
$$\bar{\nu}_e + d \to e^+ + n + n \quad (\bar{\nu} - \text{CC}), \tag{3}$$
$$\bar{\nu}_x + d \to \bar{\nu}_x + n + p \quad (\bar{\nu} - \text{NC}), \tag{4}$$

where $x = e$, μ or τ. We briefly describe our calculational framework and explain in what specific aspects we improve upon NSGK [5].

The four-momenta of the participating particles are labeled as

$$\nu/\bar{\nu}(k) + d(P) \to \ell(k') + N_1(p'_1) + N_2(p'_2), \tag{5}$$

where ℓ corresponds to $e^\pm$ for the CC reactions [Eqs. (1), (3)], and to ν or $\bar{\nu}$ for the NC reactions [Eqs. (2), (4)]. The energy–momentum conservation reads: $k + P = k' + P'$ with $P' \equiv p'_1 + p'_2$. A momentum transferred from the lepton to the two-nucleon system is denoted by $q^\mu = k^\mu - k'^\mu = P'^\mu - P^\mu$. In the laboratory system, which we use throughout this work, we write

$$\begin{aligned} &k^\mu = (E_\nu, \boldsymbol{k}), \qquad k'^\mu = (E'_\ell, \boldsymbol{k}'), \\ &P^\mu = (M_d, \boldsymbol{0}), \qquad P'^\mu = (P'^0, \boldsymbol{P}'), \qquad q^\mu = (\omega, \boldsymbol{q}). \end{aligned} \tag{6}$$

The interaction Hamiltonian for semileptonic weak processes is given by the product of the hadron current (J_λ) and the lepton current (L^λ) as

$$H_W^{\text{CC}} = \frac{G'_F V_{ud}}{\sqrt{2}} \int d\boldsymbol{x} \left[J_\lambda^{\text{CC}}(\boldsymbol{x}) L^{\text{CC},\lambda}(\boldsymbol{x}) + \text{h.c.} \right] \tag{7}$$

for the CC process and

$$H_W^{\text{NC}} = \frac{G'_F}{\sqrt{2}} \int d\boldsymbol{x} \left[J_\lambda^{\text{NC}}(\boldsymbol{x}) L^{\text{NC},\lambda}(\boldsymbol{x}) + \text{h.c.} \right] \tag{8}$$

for the NC process. Here G'_F is the weak coupling constant, and V_{ud} is the K-M matrix element. For the weak coupling constant, instead of $G_F = 1.16637 \times 10^{-5}$ GeV^{-2} employed in NSGK, we adopt here $G'_F = 1.1803 \times 10^{-5}$ GeV^{-2} obtained from $0^+ \to 0^+$

nuclear β-decays [26].[4] G'_F subsumes the bulk of the *inner* radiative corrections.[5] The K-M matrix element is taken to be $V_{ud} = 0.9740$ [26] instead of $V_{ud} = 0.9749$ used in NSGK.

The leptonic currents, $L^{\mathrm{CC},\lambda}$ and $L^{\mathrm{NC},\lambda}$, are well known. The hadronic charged current is written as

$$J_\lambda^{\mathrm{CC}}(\boldsymbol{x}) = V_\lambda^{\pm}(\boldsymbol{x}) + A_\lambda^{\pm}(\boldsymbol{x}), \tag{9}$$

where V_λ and A_λ denote the vector and axial-vector currents, respectively. The superscript $+(-)$ denotes the isospin-raising (-lowering) operator for the $\bar{\nu}(\nu)$-reaction. The hadronic neutral current is given by the standard model as

$$J_\lambda^{\mathrm{NC}}(\boldsymbol{x}) = \bigl(1 - 2\sin^2\theta_W\bigr)V_\lambda^3 + A_\lambda^3 - 2\sin^2\theta_W\, V_\lambda^s, \tag{10}$$

where θ_W is the Weinberg angle. V_λ^s is the isoscalar part of the vector current, and the superscript '3' denotes the third component of the isovector current. The hadron current consists of one-nucleon impulse approximation (IA) terms and two-body exchange current (EXC) terms.

The IA currents are given in terms of the single-nucleon matrix elements of J_λ. The standard parameterization for them is

$$\langle N(p')|V_\lambda^{\pm}(0)|N(p)\rangle = \bar{u}(p')\left[f_V\gamma_\lambda + i\frac{f_M}{2m}\sigma_{\lambda\rho}q^\rho\right]\tau^{\pm}u(p), \tag{11}$$

$$\langle N(p')|A_\lambda^{\pm}(0)|N(p)\rangle = \bar{u}(p')\bigl[f_A\gamma_\lambda\gamma^5 + f_P\gamma^5 q_\lambda\bigr]\tau^{\pm}u(p), \tag{12}$$

where m is the average of the proton and neutron masses. For the third component of the isovector current, we simply replace $\tau^{\pm}$ with $\tau^3/2$. The isoscalar current is given as

$$\langle N(p')|V_\lambda^s(0)|N(p)\rangle = \bar{u}(p')\left[f_V\gamma_\lambda + i\frac{f_M^s}{2m}\sigma_{\lambda\rho}q^\rho\right]\frac{1}{2}u(p). \tag{13}$$

As for the q_μ^2 dependence of the form factors we use the results of the latest analyses in [27,28]:

$$f_V\bigl(q_\mu^2\bigr) = G_D\bigl(q_\mu^2\bigr)(1+\mu_p\eta)(1+\eta)^{-1}, \tag{14}$$

$$f_M\bigl(q_\mu^2\bigr) = G_D\bigl(q_\mu^2\bigr)(\mu_p - \mu_n - 1 - \mu_n\eta)(1+\eta)^{-1}, \tag{15}$$

$$f_A\bigl(q_\mu^2\bigr) = -g_A\, G_A\bigl(q_\mu^2\bigr), \tag{16}$$

$$f_P\bigl(q_\mu^2\bigr) = \frac{2m}{m_\pi^2 - q_\mu^2} f_A\bigl(q_\mu^2\bigr), \tag{17}$$

$$f_M^s\bigl(q_\mu^2\bigr) = G_D\bigl(q_\mu^2\bigr)(\mu_p + \mu_n - 1 + \mu_n\eta)(1+\eta)^{-1}, \tag{18}$$

with

[4] The relation between G'_F and the quantities used in [26] is: $G'^2_F = (G_V/V_{ud})^2(1+\Delta_R^V)$, where Δ_R^V is the nucleus-independent radiative correction.

[5] To be precise, the inner corrections for the CC and NC reactions may differ but the difference reported in the literature [18] is comparable to the estimated uncertainty of our present calculation (see below).

$$G_D(q_\mu^2) = \left(1 - \frac{q_\mu^2}{0.71\text{GeV}^2}\right)^{-2}, \tag{19}$$

$$G_A(q_\mu^2) = \left(1 - \frac{q_\mu^2}{1.04\text{GeV}^2}\right)^{-2}, \tag{20}$$

where $\mu_p = 2.793$, $\mu_n = -1.913$, $\eta = -\frac{q_\mu^2}{4m^2}$ and m_π is the pion mass. For g_A, we adopt the current standard value, $g_A = 1.267$ [29], instead of $g_A = 1.254$ used in NSGK. In addition, as the axial-vector mass in Eq. (20), we use the value which was obtained in the latest analysis [28] of (anti)neutrino scattering and charged-pion electroproduction. The change in $G_A(q_\mu^2)$ is in fact not consequential for $\sigma_{\nu d}$ in the solar-ν energy region. Regarding f_P, we assume PCAC and pion-pole dominance. A contribution from this term is known to be proportional to the lepton mass, which leads to very small contribution from the induced pseudoscalar term in our case. Although deviations from the naive pion-pole dominance of f_P have been carefully studied [30], we can safely neglect those deviations here. For the IA current given above, we carry out the non-relativistic reduction in the same manner as in NSGK.

We now consider the exchange currents (EXC). The axial-vector EXC, A^μ_{EXC}, consists of a pion-pole term and a non-pole term, $\bar{A}^\mu_{\text{EXC}}$. Using the PCAC hypothesis, however, we can express A^μ_{EXC} in terms of the non-pole contribution alone:

$$A^\mu_{\text{EXC}} = \bar{A}^\mu_{\text{EXC}} - \frac{q^\mu}{m_\pi^2 - q_\mu^2}\left(\boldsymbol{q}\cdot\overline{\boldsymbol{A}}_{\text{EXC}} - \omega\bar{A}_{\text{EXC},0}\right). \tag{21}$$

We therefore need only specify a model for the non-pole terms; the total contribution of A^μ_{EXC} can be obtained with the use of Eq. (21). Regarding the space component of the axial-vector current, we employ $\boldsymbol{A}_{\text{EXC}}$ adjusted in such a manner that the experimental value of Γ_t^β be reproduced (see the discussion in Introduction). Following Schiavilla et al. [11], we consider the π-pair current (denoted by πS), ρ-pair current (ρS), π-exchange Δ-excitation current ($\Delta\pi$), ρ-exchange Δ-excitation current ($\Delta\rho$) and $\pi\rho$-exchange current ($\pi\rho$). The explicit expressions of these two-body currents (acting on the ith and jth nucleons) are as follows.

$$\begin{aligned}\overline{\boldsymbol{A}}^\pm_{ij}(\boldsymbol{q};\pi\text{S}) = {} & -\frac{f_A}{m}\frac{f_{\pi NN}^2}{m_\pi^2}\frac{\boldsymbol{\sigma}_j\cdot\boldsymbol{k}_j}{m_\pi^2+\boldsymbol{k}_j^2}f_\pi^2(\boldsymbol{k}_j)\\ & \times\left\{(\boldsymbol{\tau}_i\times\boldsymbol{\tau}_j)^\pm\boldsymbol{\sigma}_i\times\boldsymbol{k}_j - \tau_j^\pm[\boldsymbol{q}+i\boldsymbol{\sigma}_i\times(\boldsymbol{p}_i+\boldsymbol{p}_i')]\right\} + (i\rightleftharpoons j),\end{aligned} \tag{22}$$

$$\begin{aligned}\overline{\boldsymbol{A}}^\pm_{ij}(\boldsymbol{q};\rho\text{S}) = {} & f_A\frac{g_\rho^2(1+\kappa_\rho)^2}{4m^3}\frac{f_\rho^2(\boldsymbol{k}_j)}{m_\rho^2+\boldsymbol{k}_j^2}\\ & \times\Big(\tau_j^\pm\left\{(\boldsymbol{\sigma}_j\times\boldsymbol{k}_j)\times\boldsymbol{k}_j - i[\boldsymbol{\sigma}_i\times(\boldsymbol{\sigma}_j\times\boldsymbol{k}_j)]\times(\boldsymbol{p}_i+\boldsymbol{p}_i')\right\}\\ & + (\boldsymbol{\tau}_i\times\boldsymbol{\tau}_j)^\pm\left\{\boldsymbol{q}\boldsymbol{\sigma}_i\cdot(\boldsymbol{\sigma}_j\times\boldsymbol{k}_j) + i(\boldsymbol{\sigma}_j\times\boldsymbol{k}_j)\times(\boldsymbol{p}_i+\boldsymbol{p}_i')\right.\\ & \left.- [\boldsymbol{\sigma}_i\times(\boldsymbol{\sigma}_j\times\boldsymbol{k}_j)]\times\boldsymbol{k}_j\right\}\Big) + (i\rightleftharpoons j),\end{aligned} \tag{23}$$

$$\overline{\boldsymbol{A}}^{\pm}_{ij}(\boldsymbol{q};\Delta\pi) = \frac{16}{25} f_A \frac{f^2_{\pi NN}}{m^2_\pi (m_\Delta - m)} \frac{\boldsymbol{\sigma}_j \cdot \boldsymbol{k}_j}{m^2_\pi + \boldsymbol{k}^2_j} f^2_\pi(\boldsymbol{k}_j) \times \left[4\tau^{\pm}_j \boldsymbol{k}_j - (\boldsymbol{\tau}_i \times \boldsymbol{\tau}_j)^{\pm} \boldsymbol{\sigma}_i \times \boldsymbol{k}_j\right] + (i \rightleftharpoons j), \tag{24}$$

$$\overline{\boldsymbol{A}}^{\pm}_{ij}(\boldsymbol{q};\Delta\rho) = -\frac{4}{25} f_A \frac{g^2_\rho (1+\kappa_\rho)^2}{m^2 (m_\Delta - m)} \frac{f^2_\rho(\boldsymbol{k}_j)}{m^2_\rho + \boldsymbol{k}^2_j} \times \left\{4\tau^{\pm}_j (\boldsymbol{\sigma}_j \times \boldsymbol{k}_j) \times \boldsymbol{k}_j - (\boldsymbol{\tau}_i \times \boldsymbol{\tau}_j)^{\pm} \boldsymbol{\sigma}_i \times [(\boldsymbol{\sigma}_j \times \boldsymbol{k}_j) \times \boldsymbol{k}_j]\right\} + (i \rightleftharpoons j), \tag{25}$$

$$\overline{\boldsymbol{A}}^{\pm}_{ij}(\boldsymbol{q};\pi\rho) = 2 f_A \frac{g^2_\rho}{m} \frac{\boldsymbol{\sigma}_j \cdot \boldsymbol{k}_j}{(m^2_\rho + \boldsymbol{k}^2_i)(m^2_\pi + \boldsymbol{k}^2_j)} f_\rho(\boldsymbol{k}_i) f_\pi(\boldsymbol{k}_j) (\boldsymbol{\tau}_i \times \boldsymbol{\tau}_j)^{\pm} \times [(1+\kappa_\rho)\boldsymbol{\sigma}_i \times \boldsymbol{k}_i - i(\boldsymbol{p}_i + \boldsymbol{p}'_i)] + (i \rightleftharpoons j). \tag{26}$$

Here m_ρ and m_Δ are the masses of the ρ-meson, and Δ-particle, respectively; f_A is the axial form factor given in Eq. (16). The total three-momentum transfer is $\boldsymbol{q} \equiv \boldsymbol{k}_i + \boldsymbol{k}_j$, with $\boldsymbol{k}_{i(j)}$ being the momentum transferred to the ith (jth) nucleon; $\boldsymbol{p}_i$ and $\boldsymbol{p}'_i$ are the initial and final momenta of the ith nucleon. The form factors, $f_\pi(\boldsymbol{k})$ and $f_\rho(\boldsymbol{k})$, for the pion–nucleon and ρ-nucleon vertices are parametrized as

$$f_\pi(\boldsymbol{k}) = \frac{\Lambda^2_\pi - m^2_\pi}{\Lambda^2_\pi + \boldsymbol{k}^2}, \qquad f_\rho(\boldsymbol{k}) = \frac{\Lambda^2_\rho - m^2_\rho}{\Lambda^2_\rho + \boldsymbol{k}^2} \tag{27}$$

with $\Lambda_\pi = 4.8$ fm^{-1} and $\Lambda_\rho = 6.8$ fm^{-1}. The quark model has been used to relate the coupling constants of the $\pi N\Delta$, $\rho N\Delta$ and $A_\mu N\Delta$ vertices to the πNN, ρNN, and $A_\mu NN$ vertices, respectively. Schiavilla et al. [11] have pointed out that the experimental value of Γ^β_t can be reproduced if the strengths of $\overline{\boldsymbol{A}}(\Delta\pi)$ in Eq. (24) and $\overline{\boldsymbol{A}}(\Delta\rho)$ in Eq. (25) are reduced by a common factor of 0.8. We employ here the same adjustment of $\overline{\boldsymbol{A}}(\Delta\pi)$ and $\overline{\boldsymbol{A}}(\Delta\rho)$. For the third component of the isovector current, we simply replace $\tau^{\pm}_i$ and $(\boldsymbol{\tau}_i \times \boldsymbol{\tau}_j)^{\pm}$ with $\tau^3_i/2$ and $(\boldsymbol{\tau}_i \times \boldsymbol{\tau}_j)^3/2$, respectively. (The same prescription will be applied to the other exchange currents as well.) For the time component we use the one-pion exchange current (the so-called KDR current [31]), which gives the dominant EXC to $\bar{A}^{\pm}_{0ij}$. The explicit form of the KDR current, with a vertex form factor supplemented,[6] reads

$$\bar{A}^{\pm}_{0ij}(\boldsymbol{q};\mathrm{KDR}) = \frac{2}{i f_A} \left(\frac{f_{\pi NN}}{m_\pi}\right)^2 f^2_\pi(\boldsymbol{k}_j) \frac{\boldsymbol{\sigma}_j \cdot \boldsymbol{k}_j}{m^2_\pi + \boldsymbol{k}^2_j} (\boldsymbol{\tau}_i \times \boldsymbol{\tau}_j)^{\pm} + (i \rightleftharpoons j). \tag{28}$$

Regarding the vector exchange currents, we first note that the time component should be negligibly small since its contribution vanishes in the static limit. For the space component, $\boldsymbol{V}$, we take account of the pair, pionic, and isobar currents. As in NSGK, we adopt the one-pion exchange model for the pair and pionic currents and the one-pion and one-ρ-meson exchange model for the isobar current. Their explicit expressions are:

[6] For A_0 and the vector currents, we use the same form factors as in NSGK. They are parametrized as in Eq. (27), but the numerical values of Λ_π and Λ_ρ are: $\Lambda_\pi = 6.0$ fm^{-1}, $\Lambda_\rho = 7.3$ fm^{-1}.

$$\boldsymbol{V}_{ij}^{\pm}(\boldsymbol{q};\text{pair}) = -2if_V\left(\frac{f_{\pi NN}}{m_\pi}\right)^2 f_\pi^2(\boldsymbol{k}_j)\frac{\boldsymbol{\sigma}_i(\boldsymbol{\sigma}_j\cdot\boldsymbol{k}_j)}{m_\pi^2+\boldsymbol{k}_j^2}(\boldsymbol{\tau}_i\times\boldsymbol{\tau}_j)^{\pm} + (i\rightleftharpoons j), \tag{29}$$

$$\boldsymbol{V}_{ij}^{\pm}(\boldsymbol{q};\text{pionic}) = 2if_V\left(\frac{f_{\pi NN}}{m_\pi}\right)^2 f_\pi(\boldsymbol{k}_i)f_\pi(\boldsymbol{k}_j)\frac{(\boldsymbol{\sigma}_i\cdot\boldsymbol{k}_i)(\boldsymbol{\sigma}_j\cdot\boldsymbol{k}_j)(\boldsymbol{k}_i-\boldsymbol{k}_j)}{(m_\pi^2+\boldsymbol{k}_i^2)(m_\pi^2+\boldsymbol{k}_j^2)} \times(\boldsymbol{\tau}_i\times\boldsymbol{\tau}_j)^{\pm}, \tag{30}$$

$$\begin{aligned}\boldsymbol{V}_{ij}^{\pm}(\boldsymbol{q};\Delta) = -i4\pi\frac{f_V+f_M}{2m}\Bigg[&\frac{f_\pi^2(\boldsymbol{k}_j)}{m_\pi^2+\boldsymbol{k}_j^2}\boldsymbol{q} \times\left\{c_0\boldsymbol{k}_j\tau_j^{\pm}+d_1(\boldsymbol{\sigma}_i\times\boldsymbol{k}_j)(\boldsymbol{\tau}_i\times\boldsymbol{\tau}_j)^{\pm}\right\}(\boldsymbol{\sigma}_j\cdot\boldsymbol{k}_j)\\ &+\frac{f_\rho^2(\boldsymbol{k}_j)}{m_\rho^2+\boldsymbol{k}_j^2}\boldsymbol{q}\times\left\{c_\rho\boldsymbol{k}_j\times(\boldsymbol{\sigma}_j\times\boldsymbol{k}_j)\tau_j^{\pm}\right.\\ &\left.+d_\rho\boldsymbol{\sigma}_i\times\big(\boldsymbol{k}_j\times(\boldsymbol{\sigma}_j\times\boldsymbol{k}_j)\big)(\boldsymbol{\tau}_i\times\boldsymbol{\tau}_j)^{\pm}\right\}\Bigg]\\ &+(i\rightleftharpoons j).\end{aligned} \tag{31}$$

The numerical values of the various parameters are

$$\frac{f_{\pi NN}^2}{4\pi}=0.08,\qquad c_0m_\pi^3=0.188,\qquad d_1m_\pi^3=-0.044,$$
$$c_\rho m_\rho^3=36.2,\qquad d_\rho=-\frac{1}{4}c_\rho. \tag{32}$$

As discussed in NSGK, these values lead to $np\to d\gamma$ cross sections that agree with the experimental values.

Apart from the modifications explicitly mentioned above, the theoretical framework of the present calculation is the same as in NSGK [5] and, for further details of the formalism, we refer to Sections II and III of NSGK.

3. Numerical results

In reporting the numerical results of our calculation, we shall be primarily concerned with the "*standard case*",[7] which is characterized by the following features. The calculational framework of the *standard case* is the same as in NSGK except for the specific points of improvements explained above. Also, the numerical values of the input parameters in the *standard case* are identical with those used in the *standard run* in NSGK, apart from the changes explicitly mentioned in the preceding section. As for the NN interaction needed to generate the initial and final nuclear wave functions, the *standard case* employs the AV18 potential [19].[8] In what follows, we largely concentrate on the

[7] The *standard case* here should be distinguished from the *standard run* in NSGK.

[8] The use of the AV18 potential here is consistent with the fact that, in [24], the strength of $\hat{d}^R$ was determined using the 3-body wave functions obtained with the AV18 potential (and additional three-body forces). We also mention that the *standard run* in NSGK also uses the AV18 potential.

standard case and discuss other cases (to be specified as needed) only in the context of assessing the model dependence.

For the *standard case*, we have calculated the total cross sections and differential cross sections for the four reactions Eqs. (1)–(4), up to $E_\nu = 170$ MeV. In this communication, however, we concentrate on the quantities directly relevant to the SNO solar neutrino experiments and limit ourselves to the neutrino reactions (both CC and NC) for $E_\nu \leqslant 20$ MeV.[9] The $\sigma_{\nu d}$ corresponding to the *standard case* is shown in Table 1 as a function of E_ν.[10] The results given in Table 1 should supersede the corresponding results in NSGK. In the following we discuss comparison between the new and old estimates of $\sigma_{\nu d}$ as well as error estimates for the new calculation.

For clarity, when necessary, the total cross sections corresponding to the *standard case* of the present work are denoted by $\sigma_{\nu d}$(Netal), $\sigma_{\nu d}^{\rm CC}$(Netal) and $\sigma_{\nu d}^{\rm NC}$(Netal); those corresponding to the *standard run* in NSGK are denoted by $\sigma_{\nu d}$(NSGK), $\sigma_{\nu d}^{\rm CC}$(NSGK) and $\sigma_{\nu d}^{\rm NC}$(NSGK). The ratio of $\sigma_{\nu d}^{\rm CC}$(Netal) to $\sigma_{\nu d}^{\rm CC}$(NSGK) is given for several representative values of E_ν in the first column of Table 2. Similar information for $\sigma_{\nu d}^{\rm NC}$ is given in the second column. As the table indicates, $\sigma_{\nu d}^{\rm CC}$(Netal) is slightly larger than $\sigma_{\nu d}^{\rm CC}$(NSGK); the difference is $\sim 1.3\%$ for $E_\nu \sim 5$ MeV, $\sim 0.8\%$ for $E_\nu \sim 10$ MeV, and $\sim 0.4\%$ for $E_\nu \sim 20$ MeV. A similar tendency is seen for $\sigma_{\nu d}^{\rm NC}$ as well. The origins of the difference between $\sigma_{\nu d}$(Netal) and $\sigma_{\nu d}$(NSGK) will be analyzed below.

Changing the weak coupling constant from G_F to G_F' scales $\sigma_{\nu d}$ by an overall factor of $(G_F'/G_F)^2 \sim 1.02$. The effect of changing the value of g_A can also be well simulated by an overall factor, since the νd reaction at low energies is dominated by the Gamow–Teller transition and hence $\sigma_{\nu d}$ is essentially proportional to g_A^2. Thus the change of g_A from $g_A = 1.254$ to $g_A = 1.267$ enhances $\sigma_{\nu d}$ in the low-energy region by another factor of $(1.267/1.254)^2 \sim 1.02$.

In discussing the consequences of the change in $\boldsymbol{A}_{\rm EXC}$, it is convenient to introduce the terms, Models I and II. As described earlier, the *standard case* in the present calculation uses $\boldsymbol{A}_{\rm EXC}$ given in [11] and recapitulated in the preceding section. We refer to this choice of $\boldsymbol{A}_{\rm EXC}$ as Model I. Meanwhile, $\boldsymbol{A}_{\rm EXC}$ used in the *standard run* in NSGK consists of $\boldsymbol{A}(\Delta\pi)$ and $\boldsymbol{A}(\Delta\rho)$ alone, and its strength is adjusted to reproduce the $np \to \gamma d$ rate. We refer to this choice of $\boldsymbol{A}_{\rm EXC}$ as Model II. For each of Models I and II, Table 3 gives the contributions from the individual terms in A_μ as well as that from V_μ, the vector current. The table indicates that in either case the corrections to the IA values are dominated by the contributions from $\boldsymbol{A}(\Delta\pi)$ and $\boldsymbol{A}(\Delta\rho)$. To facilitate further comparison between Models I and II, we consider the ratio, ξ, defined by $\xi \equiv [\sigma_{\nu d}({\rm IA} + \boldsymbol{A}_{\rm EXC}) - \sigma_{\nu d}({\rm IA})]/\sigma_{\nu d}({\rm IA})$. Here, $\sigma_{\nu d}({\rm IA})$ is the result obtained with the IA current alone, while $\sigma_{\nu d}({\rm IA} + \boldsymbol{A}_{\rm EXC})$ represents the result obtained with the IA current plus $\boldsymbol{A}_{\rm EXC}$. Fig. 1 gives ξ for the CC reaction as a function of E_ν. The solid line shows ξ for Model I, while the dashed line gives ξ for Model II. It is seen that the contribution of $\boldsymbol{A}_{\rm EXC}$ in Model I is smaller than

[9] A more extensive account of our calculation will be published elsewhere. The full presentation of the numerical results of the present work can be found at the web site: http://nuc003.psc.sc.edu/~kubodera/NU-D-NSGK.

[10] The limited precision of our computer code causes 0.1% uncertainty in $\sigma_{\nu d}$ for $E_\nu \leqslant 20$ MeV, apart from uncertainties due to the model dependence to be discussed later in the text.

Table 1
Calculated values of $\sigma_{\nu d}^{\mathrm{CC}}$ and $\sigma_{\nu d}^{\mathrm{NC}}$ in units of cm^2. The "$-x$" in the parentheses means 10^{-x}; thus an entry like 4.579 (−48) stands for 4.579×10^{-48} cm^2

E_ν (MeV)	$\nu_e d \to e^- pp$	$\nu d \to \nu pn$	E_ν (MeV)	$\nu_e d \to e^- pp$	$\nu d \to \nu pn$
1.5	4.680 (−48)	0.000 (0)	8.8	1.911 (−42)	7.530 (−43)
1.6	1.147 (−46)	0.000 (0)	9.0	2.034 (−42)	8.070 (−43)
1.8	1.147 (−45)	0.000 (0)	9.2	2.160 (−42)	8.629 (−43)
2.0	3.670 (−45)	0.000 (0)	9.4	2.291 (−42)	9.209 (−43)
2.2	7.973 (−45)	0.000 (0)	9.6	2.425 (−42)	9.809 (−43)
2.4	1.428 (−44)	4.346 (−47)	9.8	2.565 (−42)	1.043 (−42)
2.6	2.279 (−44)	4.322 (−46)	10.0	2.708 (−42)	1.107 (−42)
2.8	3.369 (−44)	1.478 (−45)	10.2	2.856 (−42)	1.173 (−42)
3.0	4.712 (−44)	3.402 (−45)	10.4	3.007 (−42)	1.241 (−42)
3.2	6.324 (−44)	6.372 (−45)	10.6	3.164 (−42)	1.311 (−42)
3.4	8.216 (−44)	1.052 (−44)	10.8	3.324 (−42)	1.383 (−42)
3.6	1.040 (−43)	1.594 (−44)	11.0	3.489 (−42)	1.458 (−42)
3.8	1.289 (−43)	2.274 (−44)	11.2	3.658 (−42)	1.534 (−42)
4.0	1.569 (−43)	3.098 (−44)	11.4	3.832 (−42)	1.612 (−42)
4.2	1.881 (−43)	4.072 (−44)	11.6	4.010 (−42)	1.693 (−42)
4.4	2.225 (−43)	5.202 (−44)	11.8	4.192 (−42)	1.775 (−42)
4.6	2.604 (−43)	6.492 (−44)	12.0	4.379 (−42)	1.860 (−42)
4.8	3.016 (−43)	7.947 (−44)	12.2	4.570 (−42)	1.947 (−42)
5.0	3.463 (−43)	9.570 (−44)	12.4	4.766 (−42)	2.035 (−42)
5.2	3.945 (−43)	1.136 (−43)	12.6	4.966 (−42)	2.126 (−42)
5.4	4.463 (−43)	1.333 (−43)	12.8	5.171 (−42)	2.219 (−42)
5.6	5.017 (−43)	1.548 (−43)	13.0	5.380 (−42)	2.314 (−42)
5.8	5.608 (−43)	1.780 (−43)	13.5	5.923 (−42)	2.561 (−42)
6.0	6.236 (−43)	2.031 (−43)	14.0	6.495 (−42)	2.822 (−42)
6.2	6.902 (−43)	2.300 (−43)	14.5	7.095 (−42)	3.095 (−42)
6.4	7.605 (−43)	2.587 (−43)	15.0	7.724 (−42)	3.382 (−42)
6.6	8.347 (−43)	2.894 (−43)	15.5	8.383 (−42)	3.682 (−42)
6.8	9.127 (−43)	3.219 (−43)	16.0	9.071 (−42)	3.995 (−42)
7.0	9.946 (−43)	3.562 (−43)	16.5	9.789 (−42)	4.323 (−42)
7.2	1.080 (−42)	3.925 (−43)	17.0	1.054 (−41)	4.663 (−42)
7.4	1.170 (−42)	4.308 (−43)	17.5	1.131 (−41)	5.017 (−42)
7.6	1.264 (−42)	4.709 (−43)	18.0	1.212 (−41)	5.385 (−42)
7.8	1.362 (−42)	5.130 (−43)	18.5	1.296 (−41)	5.767 (−42)
8.0	1.464 (−42)	5.571 (−43)	19.0	1.383 (−41)	6.162 (−42)
8.2	1.569 (−42)	6.031 (−43)	19.5	1.474 (−41)	6.571 (−42)
8.4	1.679 (−42)	6.511 (−43)	20.0	1.567 (−41)	6.994 (−42)
8.6	1.793 (−42)	7.010 (−43)			

that in Model II by 2–4%. This difference is mainly due to the reduced strength of the Δ-excitation currents in Model I. For further discussion, we normalize ξ(Model II) for the CC reaction by an overall multiplicative factor chosen in such a manner that the normalized ξ(Model II) reproduces ξ(Model I) at the reaction threshold. This normalized result is given by the dash-dotted line in Fig. 1. We observe that the dash-dotted line exhibits a slight deviation from the solid line (Model I). This deviation reflects a slight difference in the E_ν-dependences of the $\boldsymbol{A}_{\mathrm{EXC}}$ contribution for Models I and II. The main cause of

Table 2
Comparison of the present results with those of NSGK [5]. The ratio, $\sigma_{\nu d}(\text{Netal})/\sigma_{\nu d}(\text{NSGK})$, is given for representative values of E_ν

E_ν (MeV)	$\nu_e d \to e^- pp$	$\nu d \to \nu pn$
5	1.013	1.011
10	1.008	1.006
15	1.006	1.003
20	1.004	1.001

Table 3
For Models I and II are shown the cumulative contributions to $\sigma_{\nu d}^{\text{CC}}$ from the various components in the current. The row labeled "IA" gives $\sigma_{\nu d}^{\text{CC}}$ obtained with the IA currents in A_μ and V_μ, and the next row labeled "$+\boldsymbol{V}_{\text{EXC}}$" gives $\sigma_{\nu d}^{\text{CC}}$ that includes the contributions of the IA currents and $\boldsymbol{V}_{\text{EXC}}$, the exchange current in $\boldsymbol{V}$. Similarly, an entry in the nth row (counting from the row labeled "IA") includes the coherent contributions of all the currents listed in the first n rows. The numbers in the last row are obtained with the full currents. The parenthesized number in the nth row gives the ratio, $\sigma_{\nu d}^{\text{CC}}(n\text{th row})/\sigma_{\nu d}^{\text{CC}}((n-1)\text{th row})$, which represents a factor by which $\sigma_{\nu d}^{\text{CC}}$ changes when the new term is added

$\sigma_{\nu d}^{\text{CC}}$ ($\times 10^{-42}$ cm^2)

E_ν	5 MeV	10 MeV	15 MeV	20 MeV
		Model I		
IA	0.3397 (–)	2.646 (–)	7.526 (–)	15.23 (–)
$+\boldsymbol{V}_{\text{EXC}}$	0.3401 (1.001)	2.654 (1.003)	7.560 (1.005)	15.33 (1.006)
$+\pi\Delta$	0.3474 (1.022)	2.719 (1.025)	7.758 (1.026)	15.74 (1.027)
$+\rho\Delta$	0.3448 (0.992)	2.695 (0.991)	7.687 (0.991)	15.59 (0.991)
$+\pi S$	0.3456 (1.002)	2.702 (1.003)	7.707 (1.003)	15.63 (1.003)
$+\rho S$	0.3447 (0.997)	2.694 (0.997)	7.682 (0.997)	15.58 (0.997)
$+\pi-\rho$	0.3463 (1.005)	2.708 (1.005)	7.724 (1.005)	15.67 (1.006)
$+A_{\text{EXC}}^0$	0.3463 (1.000)	2.708 (1.000)	7.724 (1.000)	15.67 (1.000)
		Model II		
IA	0.3397 (–)	2.646 (–)	7.526 (–)	15.23 (–)
$+\boldsymbol{V}_{\text{EXC}}$	0.3401 (1.001)	2.654 (1.003)	7.560 (1.005)	15.33 (1.006)
$+\pi\Delta$	0.3612 (1.062)	2.841 (1.071)	8.128 (1.075)	16.52 (1.078)
$+\rho\Delta$	0.3567 (0.988)	2.801 (0.986)	8.007 (0.985)	16.26 (0.985)
$+A_{\text{EXC}}^0$	0.3567 (1.000)	2.801 (1.000)	8.008 (1.000)	16.26 (1.000)

this difference can be traced as follows. From Table 3 we can deduce that the dominant contributions coming from the Δ-excitation currents have almost the same E_ν-dependence for Models I and II, although their absolute values differ for the two models. On the other hand, the contributions of $\boldsymbol{A}(\pi S)$, $\boldsymbol{A}(\rho S)$ and $\boldsymbol{A}(\pi\rho)$, which are included only in Model I, are virtually E_ν-independent, and their magnitudes are small. These features lead to the slightly weaker E_ν-dependence in $\boldsymbol{A}_{\text{EXC}}$(Model I) than in $\boldsymbol{A}_{\text{EXC}}$(Model II). The behavior of ξ for the NC reaction (not shown) is similar to ξ for the CC reaction.

The error estimate adopted in NSGK essentially consists in taking the difference between Models I and II as a typical measure of model dependence. As mentioned in the

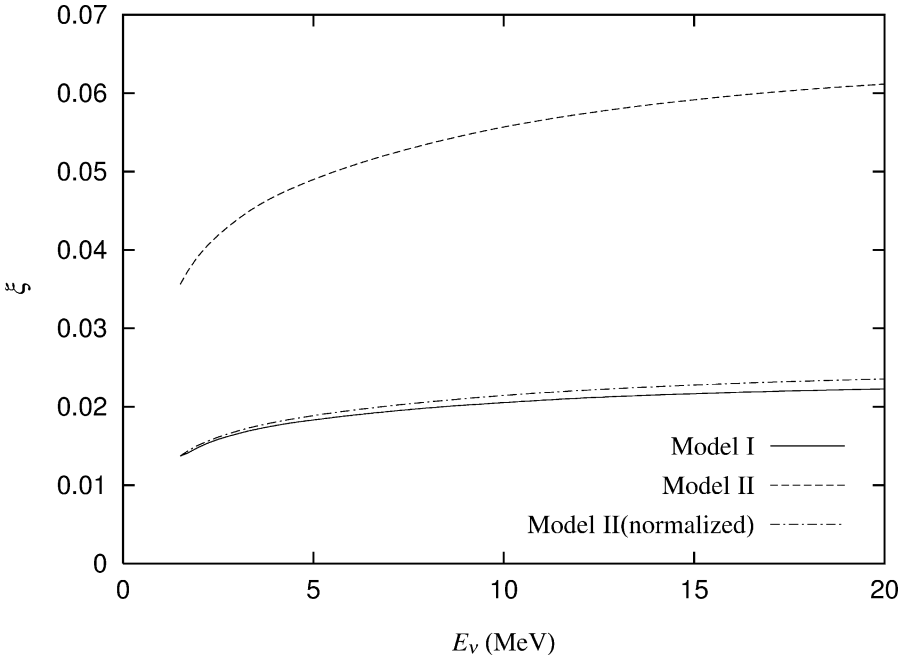

Fig. 1. Contributions of $\boldsymbol{A}_{\rm EXC}$ to $\sigma_{\nu d}^{\rm CC}$; ξ defined in the text is plotted for Model I (solid line) and Model II (dashed line). The dash-dotted line represents the "normalized" version of Model II described in the text.

introduction, however, Model II, which fails to explain Γ_t^β, should not be given the same status as Model I. To attain a more reasonable estimate of the theoretical uncertainty, we propose the following interpretation of the feature seen in Fig. 1. The fact that Model I has been adjusted to reproduce Γ_t^β means that it can yield model-independent results at a specific kinematics but that, without additional experimental information, the E_ν-dependence of $\sigma_{\nu d}$ cannot be fully controlled. This uncertainty may be assessed from the difference between the solid and dash-dotted lines in Fig. 1. From this argument we assign 0.2% uncertainty to the contribution of $\boldsymbol{A}_{\rm EXC}$ to $\sigma_{\nu d}$ in the solar neutrino energy range, $E_\nu < 20$ MeV.

We recapitulate our discussion regarding the change from $\sigma_{\nu d}$(NSGK) to $\sigma_{\nu d}$(Netal): a $\sim$4% enhancement of $\sigma_{\nu d}$ due to the changes in the Fermi constant and g_A and a $\sim$ 3% reduction due to the use of the new $\boldsymbol{A}_{\rm EXC}$ (Model I) that reproduces Γ_t^β. These two changes partially cancelling each other, the net result is the enhancement of $\sigma_{\nu d}$ by $\sim$ 1%, and this is what is seen in Table 2.

As mentioned earlier, an additional important measure of reliability of our SNPA calculation is obtained by comparing it with the results of an EFT* calculation by Ando et al. [25]. By using the value of the low-energy constant, $\hat{d}^R$, fixed to reproduce the experimental value of Γ_t^β [24], Ando et al. [25] have carried out a parameter-free EFT-motivated calculation of $\sigma_{\nu d}$. Although the cut-off regularization method used in [25] can introduce the cut-off dependence into the formalism, it has been checked [25] that this

Table 4
Comparison of SNPA and EFT calculations. The ratio, $\eta \equiv \sigma_{\nu d}(\text{EFT*})/\sigma_{\nu d}(s\text{-wave})$, is given for representative values of E_ν

E_ν (MeV)	$\nu_e d \to e^- pp$	$\nu d \to \nu pn$
5	1.003	1.004
10	1.001	1.003
15	0.999	1.002
20	0.998	1.001

Table 5
Dependence of $\sigma_{\nu d}^{\text{NC}}$ on NN potentials. 'Bonn' and 'AV18' represent the results obtained with the CD-Bonn and the AV18 potentials, respectively

$\sigma_{\nu d}^{\text{NC}}$ ($\times 10^{-42}$ cm^2)

E_ν	5 MeV		10 MeV		15 MeV		20 MeV	
	Bonn	AV18	Bonn	AV18	Bonn	AV18	Bonn	AV18
IA	0.09459	0.09390	1.091	1.083	3.327	3.300	6.871	6.814
IA + EXC	0.09557	0.09570	1.104	1.107	3.373	3.382	6.973	6.994

dependence is negligibly small for a physically reasonable range of the cut-off parameter; the relative variation in $\sigma_{\nu d}$ only amounts to 0.02%, which is much smaller than the above-mentioned 0.2% uncertainty inherent in our SNPA calculation. In fact, the uncertainty in $\sigma_{\nu d}$ obtained by Ando et al. is dominated by the 0.5% error resulting from the uncertainty in the experimental value of Γ_t^β. We now compare $\sigma_{\nu d}$(Netal) with $\sigma_{\nu d}$(EFT*) obtained in the EFT* calculation of Ando et al. [25]. Since Ref. [25] only includes the s-wave of the final NN state, we compare $\sigma_{\nu d}$(EFT*) with $\sigma_{\nu d}(s\text{-wave})$, which represents the s-wave contribution to $\sigma_{\nu d}$ calculated for the *standard case*. The ratio, $\eta \equiv \sigma_{\nu d}(\text{EFT*})/\sigma_{\nu d}(s\text{-wave})$, is shown in Table 4, from which we can conclude that SNPA and EFT give identical results at the 1% level.

We proceed to consider the NN potential dependence. As mentioned, the CD-Bonn potential is somewhat distinct from the potentials considered in NSGK, in that it has a significantly smaller D-state probability; $P_D(\text{CD-Bonn}) = 4.2\%$ as compared with $P_D(\text{AV18}) = 5.8\%$. We compare in Table 5 the $\sigma_{\nu d}^{\text{NC}}$ obtained with the AV18 and CD-Bonn potentials. The difference between the two cases is found to be practically negligible. With the CD-Bonn potential, because of its larger S-state probability, the contribution from the IA current becomes larger, whereas the contribution from $\boldsymbol{A}_{\text{EXC}}$ is smaller due to its reduced D-state probability. Our explicit calculation demonstrates that the cancellation between these two opposing tendencies is almost perfect, providing a yet another manifestation of the robustness of the calculated $\sigma_{\nu d}$. A similar stabilizing mechanism was noticed by Schiavilla et al. in their study of the pp-fusion cross section [11].

Apart from the absolute values of $\sigma_{\nu d}^{\text{CC}}$ and $\sigma_{\nu d}^{\text{NC}}$, the ratio, $R \equiv \sigma_{\nu d}^{\text{NC}}/\sigma_{\nu d}^{\text{CC}}$, is also an important quantity for SNO experiments. As emphasized by Bahcall and Lisi [32], a measurement at SNO of the ratio of the number of the NC to CC events (the NC/CC ratio) would place stringent constraints on various neutrino oscillation scenarios. Since

Table 6
The ratio, $R \equiv \sigma(\nu d \to \nu np)/\sigma(\nu_e d \to e^- pp)$, calculated for representative values of E_ν. The second column gives $R_{\rm stnd}$ corresponding to the *standard case*. The third, fourth and fifth columns give $R_{\rm IA}/R_{\rm stnd}$, $R_{\rm [Model\ II]}/R_{\rm stnd}$ and $R_{\rm [EFT^*]}/R_{\rm stnd}$, respectively. Here $R_{\rm IA}$ corresponds to R obtained with the IA current alone, while $R_{\rm [Model\ II]}$ and $R_{\rm [EFT^*]}$ corresponds to Model II and EFT*, respectively

E_ν (MeV)	$R_{\rm stnd}$	IA	Model II	EFT*
5	0.2764	1.000	1.004	1.001
10	0.4087	1.001	1.004	1.002
15	0.4378	1.002	1.004	1.004
20	0.4464	1.002	1.005	1.004

the precision of the predicted value of the NC/CC ratio is affected by the uncertainty in R (see Fig. 7 in [32]), we discuss the model dependence of R. Table 6 gives the values of R calculated for the various cases discussed above. The table indicates that the model dependence of R is smaller than that of $\sigma_{\nu d}^{\rm CC}$ and $\sigma_{\nu d}^{\rm NC}$ themselves. The simple IA calculation gives a value of R that agrees with $R_{\rm stnd}$ within 0.2%. The variance between the *standard case* and Model II is less than 0.5%—it is to be recalled that Model II is a rather extreme case. Furthermore, the difference between the *standard case* and the EFT* calculation does not exceed 0.4%. We therefore consider it reasonable to assign 0.5% accuracy to R. This is an improvement by a factor of ~ 2 over the precision reported in [4,5].

The stability of R can be understood as follows. We first note the following two features. (1) The contribution of the isoscalar current, which only participates in the NC reaction, is negligibly small in our case; (2) Although the iso-vector and axial-vector currents enter in different ways into the nuclear currents responsible for the CC or NC reactions, the contribution of the vector current is much smaller than that of the axial-vector current in the solar neutrino energy regime. As a consequence of these two facts, the transition operators for the NC and CC reactions in the present case are, to good accuracy, related by a rotation in isospin space. So, if there were no isospin breaking effects in the nuclear wave functions, the CC and NC transition amplitudes would be simply related by the Wigner–Eckart theorem in isospin space, leading to the complete model independence of R. In reality, there are isospin-breaking effects in the two-nucleon wave functions, but these "*external effects*" are expected to be under good control so long as one uses high-quality NN potentials that reproduce the NN data accurately.

4. Discussion and summary

Although we do not directly address the issue of radiative corrections (RC) here, we make a few remarks on it. RC can affect $\sigma_{\nu d}$ at the level of a few percent. According to Kurylov et al. [18], RC increases $\sigma_{\nu d}^{\rm CC}$ by 4% at low E_ν and by 3% at the higher end of the solar neutrino energy, while RC leads to an E_ν-independent increase of $\sigma_{\nu d}^{\rm NC}$ by $\sim 1.5\%$. The RC for $\sigma_{\nu d}^{\rm CC}$ consists of the "inner" and "outer" corrections. The former is sensitive to hadronic dynamics but energy-independent, while the latter is largely independent of hadronic dynamics but has energy-dependence. The use of experimental value of G_F' [26]

obtained from $0^+ \to 0^+$ nuclear β-decays allows one to take account of the bulk of the "inner" corrections. To obtain reasonable up-to-date estimates of the remaining "outer" corrections, we may proceed as follows. For $\sigma_{\nu d}^{\rm CC}$, we may adopt as the "outer" correction the difference between the result of Kurylov et al. (4–3%) and the estimated "inner" corrections (2.4%). For $\sigma_{\nu d}^{\rm NC}$, there is no "outer" corrections at the level of precision of this article. In adopting this prescription, we are leaving unaddressed a delicate issue of the possible difference between RC for the single nucleon and RC for multi-nucleon systems, but this seems to be the best we can do at present.

To summarize, we have improved NSGK's calculation [5] for the νd reactions by updating some of its inputs and with the use of the axial-vector exchange current the strength of which is controlled by Γ_t^β. We have also taken into account the results of a recent parameter-free EFT* calculation [25]. The new value of $\sigma_{\nu d}$, denoted by $\sigma_{\nu d}$(Netal), is slightly larger than $\sigma_{\nu d}$(NSGK) reported in [5]; $\sigma_{\nu d}$(Netal)/$\sigma_{\nu d}$(NSGK) $\sim$ 1.01. Based on the arguments presented above, we consider it reasonable to assign 1% uncertainty to $\sigma_{\nu d}$(Netal) given in Table 1, and $\sim 0.5\%$ uncertainty to R. The results in Table 1, however, do not include radiative corrections except for those already incorporated into the empirical value of G_F', which subsumes the bulk of the inner radiative corrections for nuclear β-decay. With the inclusion of the remaining radiative corrections, $\sigma_{\nu d}^{\rm CC}$ is likely to become larger than $\sigma_{\nu d}^{\rm CC}$(Netal) by up to $\sim 2\%$, while $\sigma_{\nu d}^{\rm NC}$ is expected to lie within the quoted $\sim 1\%$ error of $\sigma_{\nu d}^{\rm NC}$(Netal).

Acknowledgements

We are grateful to J. Beacom for his useful criticism on Ref. [5] and for calling our attention to the importance of the radiative corrections. Thanks are also due to John Bahcall for his interest in and useful comments on this work. We are deeply indebted to R. Machleidt for his generosity in allowing us to use his CD-Bonn potential code. This work is supported in part by the US National Science Foundation, Grant No. PHY-9900756 and No. INT-9730847, and also by the Japan Society for the Promotion of Science, Grant No. (c) 12640273.

References

[1] SNO Collaboration, Phys. Lett. B 194 (1987) 321, and references therein.
[2] Q. Ahmad et al., Phys. Rev. Lett. 87 (2001) 071301.
[3] N. Tatara, Y. Kohyama, K. Kubodera, Phys. Rev. C 42 (1990) 1694;
S. Ying, W.C. Haxton, E.M. Henley, Phys. Rev. C 45 (1992) 1982.
[4] For a review, see: K. Kubodera, S. Nozawa, Int. J. Mod. Phys. E 3 (1994) 101.
[5] S. Nakamura, T. Sato, V. Gudkov, K. Kubodera, Phys. Rev. C 63 (2001) 034617.
[6] M. Butler, J.-W. Chen, Nucl. Phys. A 675 (2000) 575;
M. Butler, J.-W. Chen, X. Kong, Phys. Rev. C 63 (2001) 035501.
[7] S. Fukuda et al., Phys. Rev. Lett. 86 (2001) 5651.
[8] M. Chemtob, M. Rho, Nucl. Phys. A 163 (1971) 1.
[9] For a recent review, see: J. Carlson, R. Schiavilla, Rev. Mod. Phys. 70 (1998) 743.

[10] J. Carlson, D.O. Riska, R. Schiavilla, R.B. Wiringa, Phys. Rev. C 44 (1991) 619.
[11] R. Schiavilla, V.G.J. Stoks, W. Glöckle, H. Kamada, A. Nogga, J. Carlson, R. Machleidt, V.R. Pandharipande, R.B. Wiringa, A. Kievsky, S. Rosati, M. Viviani, Phys. Rev. C 58 (1998) 1263.
[12] S. Weinberg, Phys. Lett. B 251 (1990) 288;
S. Weinberg, Nucl. Phys. B 363 (1991) 3.
[13] E. Epelbaum, W. Glöckle, U.-G. Meißner, Nucl. Phys. A 671 (2000) 295;
E. Epelbaum, H. Kamada, A. Nogga, H. Witała, W. Glöckle, U.-G. Meißer, Phys. Rev. Lett. 86 (2001) 4787.
[14] For a review, see: U. van Kolck, Prog. Part. Nucl. 43 (1999) 337;
S.R. Beane et al., in: M. Shifman (Ed.), At the Frontiers of Particle Physics, Handbook of QCD, Vol. 1, World Scientific, Singapore, 2001.
[15] D.B. Kaplan, M.J. Savage, M.B. Wise, Nucl. Phys. B 478 (1996) 629;
D.B. Kaplan, M.J. Savage, M.B. Wise, Phys. Lett. B 424 (1998) 390.
[16] J.F. Beacom, S.J. Parke, Phys. Rev. D 64 (2001) 091302;
J.F. Beacom, private communication.
[17] I.S. Towner, Phys. Rev. C 58 (1998) 1288.
[18] A. Kurylov, M.J. Ramsey-Musolf, P. Vogel, nucl-th/0110051.
[19] R.B. Wiringa, V.G.J. Stoks, R. Schiavilla, Phys. Rev. C 51 (1995) 38.
[20] V.G.J. Stoks, R.A.M. Klomp, C.P.F. Terheggen, J.J. de Swart, Phys. Rev. C 49 (1994) 2950.
[21] R. Machleidt, Phys. Rev. C 63 (2001) 024001.
[22] T.-S. Park, D.-P. Min, M. Rho, Phys. Rev. Lett. 74 (1995) 4153.
[23] T.-S. Park, K. Kubodera, D.-P. Min, M. Rho, Nucl. Phys. A 684 (2001) 101, and references therein.
[24] T.-S. Park, L.E. Marcucci, R. Schiavilla, M. Viviani, A. Kievsky, S. Rosati, K. Kubodera, D.-P. Min, M. Rho, nucl-th/0106025;
T.-S. Park, L.E. Marcucci, R. Schiavilla, M. Viviani, A. Kievsky, S. Rosati, K. Kubodera, D.-P. Min, M. Rho, nucl-th/0107012.
[25] S. Ando et al., in preparation.
[26] I.S. Towner, J.C. Hardy, in: P. Herczeg, C.M. Hoffman, H.V. Klapdor-Kleingrothaus (Eds.), Physics Beyond the Standard Model, World Scientific, Singapore, 1999, p. 338.
[27] M. Gourdin, Phys. Rep. 11 (1974) 29.
[28] V. Bernard, L. Elouadrhiri, U.-G. Meißner, J. Phys. G 28 (2002) R1.
[29] D.E. Groom et al., Eur. Phys. J. C 15 (2000) 1.
[30] S.L. Adler, Y. Dothan, Phys. Rev. 151 (1966) 1267;
L. Wolfenstein, in: S. Devons (Ed.), High-Energy Physics and Nuclear Structure, Plenum, New York, 1970, p. 661;
V. Bernard, N. Kaiser, U.-G. Meißner, Phys. Rev. D 50 (1994) 6899.
[31] K. Kubodera, J. Delorme, M. Rho, Phys. Rev. Lett. 40 (1978) 755.
[32] J.N. Bahcall, E. Lisi, Phys. Rev. D 54 (1996) 5417.